SEISMIC WAVEFORM DATA ANALYSIS OF SEISMIC NETWORK STATIONS OF ISLAMABAD, PESHAWAR AND LAHORE, PAKISTAN

By

MUHAMMAD UMAR

UMER ASIF

Department of Earth and Environmental Sciences

Bahria University, Islamabad.

2026

SEISMIC WAVEFORM DATA ANALYSIS OF SEISMIC NETWORK STATIONS OF ISLAMABAD, PESHAWAR AND LAHORE, PAKISTAN

A thesis submitted to Bahria University, Islamabad in partial fulfillment of the requirement for the degree of B.S in Geophysics

MUHAMMAD UMAR

UMER ASIF

Department of Earth and Environmental Sciences

Bahria University, Islamabad.

2026

ABSTRACT

Pakistan is one of the most seismically dynamic nations on the planet. It is surrounded by several active fault zones due to which earthquakes are a frequent activity in Pakistan. Pakistan Meteorological Department Seismology Division is responsible for keeping a record of these events. The primary goal of this research project is to trace these events and separate them from the noise. After that separation, different calculations will be applied to check the quality of seismic data obtained from three different stations of Islamabad, Lahore, and Peshawar.

ACKNOWLEDGEMENTS

We express our gratitude to Allah for enabling us to successfully complete our research. I would like to sincerely thank Dr. Adil Naseer, Assistant Professor in the Department of Earth and Environmental Sciences at Bahria University Islamabad, for his valuable guidance and supervision throughout our research work. Furthermore, we appreciate his facilitation in establishing collaboration with the Pakistan Meteorological Department, which played a crucial role in the completion of our thesis and served as a source of motivation.

We are thankful to Dr. Syed Umair Ullah Jamil, Head of Department Earth and Environmental Sciences at Bahria University, Islamabad, for his assistance. We are also grateful to Mr. Nasir Mehmood, National Seismic Monitoring Section, Pakistan Meteorological Department (Government of Pakistan), for their help and support. Finally, we extend our heartfelt appreciation to Mr. Muhammad Najeeb, Director, Pakistan Meteorological Department, Islamabad, for his unwavering support, insightful guidance, and invaluable contributions, which played a significant role in the successful completion of this research.

CONTENTS

CHAPTER 3

ANALYSIS OF WAVEFORM DATA

CHAPTER 4

EVENTS INTERPRETATION

LIST OF FIGURES

CHAPTER 1
INTRODUCTION

1.0 Introduction

1.1 Earthquake Seismology

Seismology is the branch of geophysics that studies earthquakes and the propagation of seismic waves through and around the Earth. A scientist specializing in this field is known as a seismologist. Earthquake seismology is one of the most effective methods for investigating the Earth's internal structure. When a seismic event, such as a natural earthquake or an artificial explosion, occurs, it releases energy in the form of elastic waves that travel through the Earth. These seismic waves are detected and recorded by instruments called seismometers, and the resulting records, known as seismograms, are used to measure and analyze ground motion.

1.2 Seismic Waves

An earthquake occurs when accumulated stress within the Earth's crust is suddenly released due to the rupture or movement along a fault zone. This release of energy generates seismic waves that propagate through the Earth's interior and across its surface. Seismic waves are broadly classified into body waves and surface waves. Body waves travel through the Earth's interior and are characterized by relatively high velocities. They are further divided into two types: Primary (P) waves and Secondary (S) waves. P-waves are compressional waves and are the first to arrive at a seismic station due to their high velocity. In contrast, S-waves are shear waves that travel more slowly than P-waves and cannot propagate through liquids.

Surface waves travel along the Earth's surface and generally have lower velocities but larger amplitudes than body waves, making them the most destructive type of seismic wave during an earthquake. Surface waves are further classified into Love waves and Rayleigh waves (Bolt, 1985).

1.3 Pakistan Meteorological Department

The Pakistan Meteorological Department (PMD) is the national organization responsible for providing meteorological and seismological services across Pakistan. Operating under the administrative control of the Aviation Division, PMD plays a vital role in collecting, analyzing, and disseminating meteorological and seismic information to support disaster management, public safety, scientific research, and various operational activities.

One of the primary responsibilities of PMD is the continuous monitoring and recording of seismic activity throughout the country. The department maintains a network of seismic stations to detect earthquakes, analyze seismic data, and archive earthquake records for future research. In addition, PMD conducts seismic hazard assessments and issues timely information and warnings related to significant earthquakes and tsunami threats whenever necessary.

For this study, seismic waveform data provided by PMD were carefully examined, and several significant local and teleseismic events were selected for detailed analysis. The selected dataset includes three earthquakes originating from the Hindu Kush region, one event from Balochistan, three events associated with the Main Boundary Thrust (MBT), and one event from the Murray Ridge in the Arabian Sea. These earthquakes were recorded at the Islamabad, Peshawar, and Lahore seismic stations of the Pakistan Seismic Network. Although all three stations successfully recorded the selected events, variations in waveform quality and signal characteristics were observed among the stations. Therefore, the primary objective of this study was to evaluate and compare the quality of seismic waveform data recorded at these three seismic network stations. The location map of the selected earthquake events and seismic stations was prepared using the Generic Mapping Tool (GMT) with the courtesy of the Pakistan Meteorological Department.

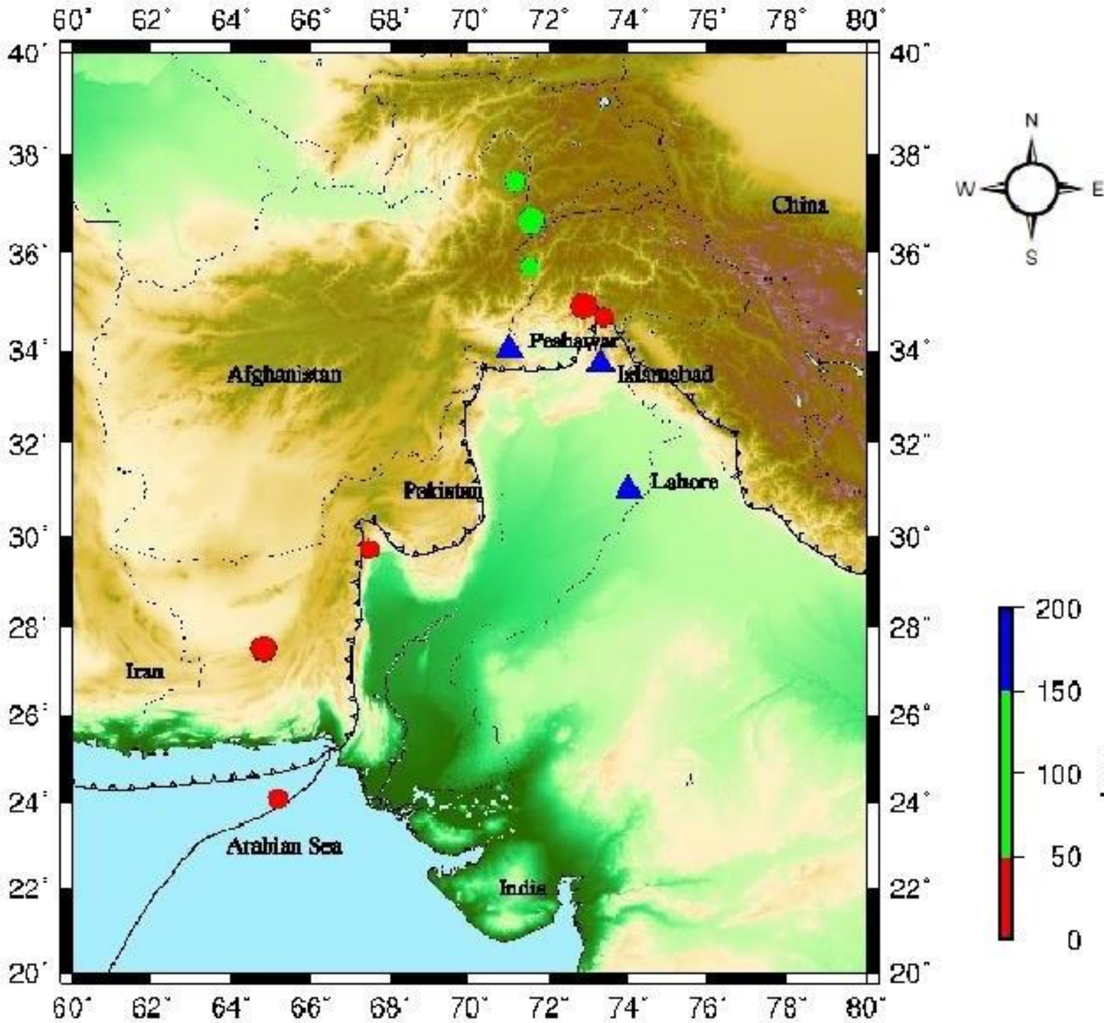

Figure.1.1. Location of three PMD Seismic Network Stations, Islamabad, Lahore and Peshawar and Earthquake epicenters used for this study. (Generic mapping tool)

1.4 Objectives

The main objectives of our research study are.

1. To separate events from noise.
2. To calculate the distance between the station and the source.
3. To calculate the ray parameter or slowness.
4. Performing H/V horizontal to vertical analysis using Geopsy.

5. To analyze the earthquakes with identification of travel time phases with residuals root mean square (R.M.S) to check the quality of stations waveform data.

1.5 Available Data

Provision of Main Data was done by Pakistan Meteorological Department. This information contained seismograms of all the events and noise, recorded at Lahore, Islamabad and Peshawar stations that occurred from 4^{th} April 2017 till 26^{th} July 2017. The provided events were in three axes North- South (n), East-West (e) and Vertical axis (z).

It is not necessary that the ground shake only in one direction. The three axes always provide a clear picture of the events. As the seismic waves travel in different trends, their motion forms a peculiarity and this peculiarity helps in identifying S from P waves, for instance, in an event, if the P-wave is traveling in a North-South trend and S- wave is shaking the ground in East-West direction then the waves will exhibit a strong motion on the n-axis and e-axis, respectively (Capon and Members, IEEE, 1969). Therefore, all three axes are taken into consideration before analyzing the seismogram for accuracy and precision in further interpretation.

1.6 Methodology for Seismic Data Processing

The methodology consists of a step-by-step workflow for processing seismic data, including data preparation, event detection, arrival-time picking, travel-time analysis, and H/V spectral analysis**.**

Observing the Acquired Data

↓

Sorting Data

↓

Tracing the Events

↓

Separating from Noise

↓

Calculating S and P - Arrivals

↓

Calculating Distance and Duration

↓

Calculating P - Waves Travel Time

↓

Determining Residual root mean square (R.M.S)

↓

H/V (Horizontal to Vertical) Analysis to Generate Noise Spectrum

CHAPTER 2
REGIONAL GEOLOGY AND TECTONIC FRAMEWORK

2.1 Geological Setting of Islamabad

The geology of the Islamabad region is primarily controlled by the ongoing convergence of the Indian and Eurasian tectonic plates. The collision between these plates, which began millions of years ago, has resulted in complex geological structures and stratigraphic sequences throughout the region. As a consequence of this tectonic activity, the Islamabad area has developed a diverse geological framework that reflects continuous deformation and crustal uplift. Based on their geological characteristics, the region can be divided into three major tectono-stratigraphic zones trending generally east-northeast, reflecting a structural orientation of approximately S. 20° E (Naeem and Bhatti, 1985).

1. The Margalla Hills in the northern region consist of a geological formation ranging from Jurassic to Eocene, comprising limestone and shale that exhibit intricate folding and thrusting along the Hazara fault zone. The uplifting of these mountains has created a significant topographic barrier over the past 1 million years (Naeem and Bhatti, 1985).
2. South of these mountains, there is a piedmont slope slanting towards the south, known as the piedmont crease belt. This area is primarily characterized by compressed folds in the sandstone and shale formations of the Rawalpindi Group (Naeem and Bhatti, 1985).
3. In the southernmost part of the region, the Soan River predominantly follows the course of the Soan syncline axis. (Naeem and Bhatti, 1985).

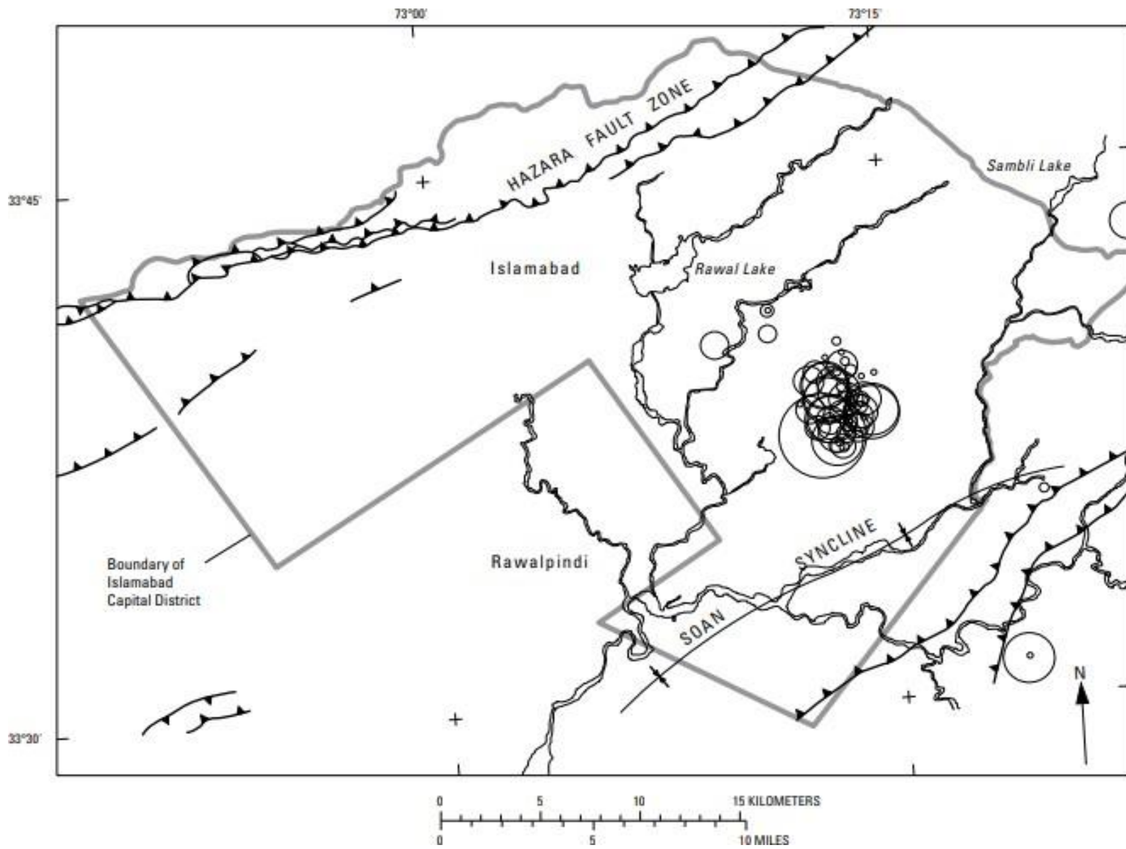

Figure 2.1. Geological map of Islamabad (Adhami et al., 1980)

2.2 Seismic Risk

The area is extensively covered by structurally deformed Quaternary deposits, reflecting the continuous effects of tectonic deformation. Historical evidence indicates that a major earthquake, estimated to have reached Modified Mercalli Intensity (MMI) IX, occurred around 25 A.D., causing the destruction of the Buddhist monasteries at Taxila, located approximately 25 km west-northwest of Islamabad. In more recent history, a magnitude 5.8 earthquake occurred on 14 February 1977, with its epicenter located about 7 km northeast of Rawalpindi. The earthquake produced a maximum intensity of Modified Mercalli Intensity (MMI) VII near the epicentral region and caused considerable structural damage, emphasizing the seismic vulnerability of the Islamabad–Rawalpindi area (Adhami et al., 1980).

2.3 Geological Setting of Peshawar

Peshawar station lies in the core of Peshawar basin. The geography and structural setting nearby Peshawar basin are extremely perplexing. The Peshawar basin lies 150 km north of the dynamic front of Himalayan deformation at the Salt Range and 50 km south of the MMT, the suture between the Indian plate and the Kohistan Island arc terrain. Between the Panjal-Khairabad fault and the MMT, the Peshawar basin covers about 5500 km2. The largest part of the basin is covered by Plio-Pleistocene basin fill with a Precambrian to Mesozoic sequence underlying it (Kazmi and Jan 1997). Between 2.8 and 0.6 Ma, the lacustrine and fluvial deposits of the Peshawar basin fill continued to be deposited. The boundaries of the basin are not well defined. Generally, the southern part has meta-Sediments while the northern part contains fracture related plutonic-volcanic rocks (Hussain and Yeat, 1989).

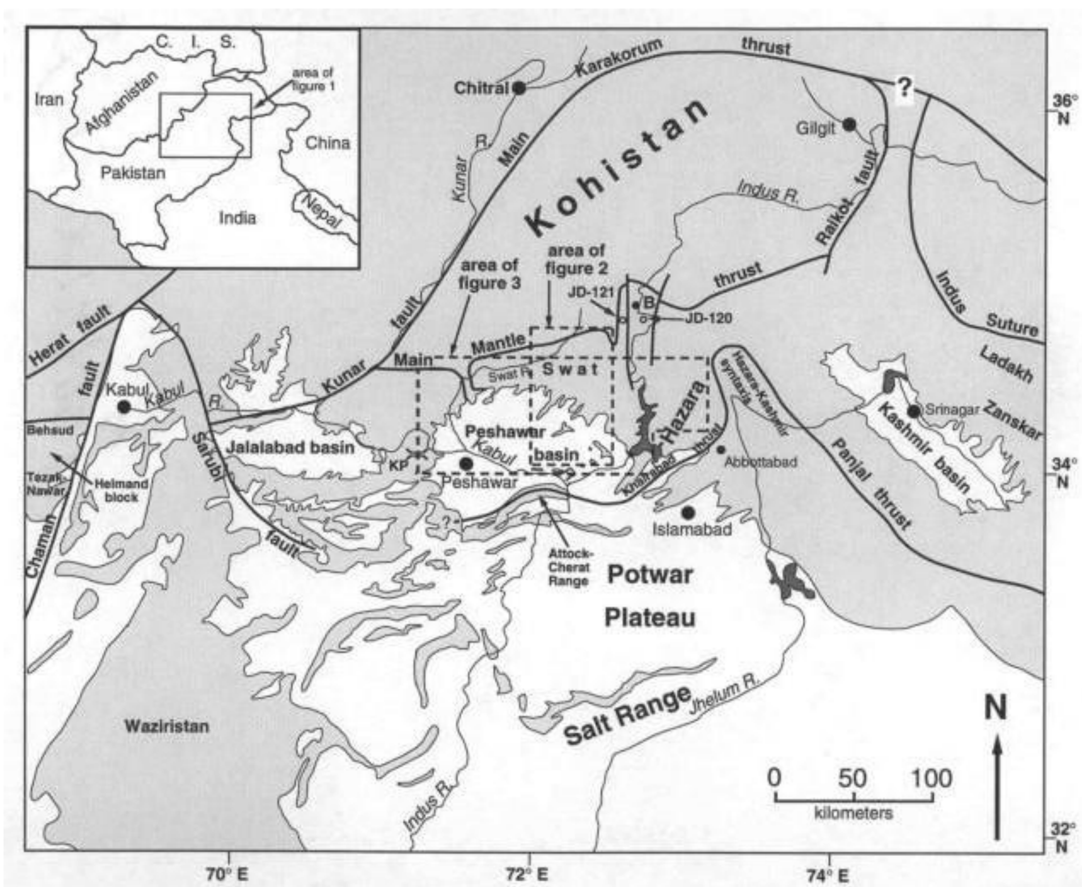

Figure 2.2. Map of Peshawar basin and vicinity (Survey of Pakistan, 1989).

2.4 Seismic Risk

Peshawar is located within the western Himalayan region, which is characterized by a high level of seismic activity due to its complex tectonic setting. The city lies in close proximity to several major active fault systems, including the Main Boundary Thrust (MBT), Main Mantle Thrust (MMT), and Main Karakoram Thrust (MKT). The Main Boundary Thrust is particularly significant, as it was associated with the devastating 2005 Kashmir earthquake. Reactivation of these major fault systems poses a considerable seismic hazard to the region, making Peshawar highly susceptible to future earthquake events (Lisa and Khawaja, 2002).

2.5 Geological Setting of Lahore

The topography of Lahore is relatively flat due to its location on the Punjab Platform. The city is situated within the Bari Doab, an extensive alluvial plain formed by the deposition of sediments carried by the Indus River and its tributaries. The term "doab" refers to the land situated between two rivers. Bari Doab is bounded by the Ravi and Chenab rivers to the northwest and west, while the Sutlej River forms its southeastern boundary. The northeastern extent of the Bari Doab approaches the foothills of the Himalayan mountain range. The region is predominantly composed of unconsolidated alluvial deposits, which have accumulated over geological time through continuous fluvial processes (Naseem and Ghulam, 2011).

2.6 Seismic Risk

The Punjab plain, where the project site is located, has low to moderate seismic activity. The project area has previously experienced intense shaking because of Himalayan earthquakes. The Main Boundary Thrust (MBT), the primary active fault of the Himalayas, is located approximately 180 km northeast of Lahore along the Himalayan front. Over the previous century, this fault has recorded earthquakes with magnitudes greater than 8. The subterranean fissures in the basement rocks, which are hidden by dense alluvial deposits, are linked to the epicenters of low to moderate magnitude earthquakes that have been seen in the Punjab plain (Shah et al., 2008).

CHAPTER 3
ANALYSIS OF WAVEFORM DATA

3.1 Introduction

Seismogram interpretation is a fundamental step in earthquake analysis. It is used to identify seismic events and determine important parameters such as P- and S-wave arrival times, epicentral distance, event duration, focal depth, travel time, slowness, and residual time. These parameters provide essential information for accurately locating and characterizing earthquake events.

After these parameters are obtained, the seismic data are processed using spectral analysis techniques. These include Horizontal to vertical (H/V (Horizontal to Vertical)) spectral ratio analysis and Frequency–Wavenumber (F-K) analysis to evaluate waveform characteristics.

The calculation of these parameters and the analysis procedures are presented step by step according to the methodology described in Chapter 1.

3.2 Methodology

3.3 Observation of Acquired Data.

The provided seismic data were in GCF format and were continuously recorded from 4 April 2017 to 26 July 2017. The dataset contained both earthquake events and background noise. Therefore, the first step was to distinguish seismic events from noise using Scream 4.5, which supports the GCF file format.

The data were organized into three separate folders representing the North–South, East–West, and Vertical components. Since ground motion occurs simultaneously in all three directions, the corresponding seismograms for each event were combined and examined as a single record to facilitate accurate identification and interpretation of the seismic signals.

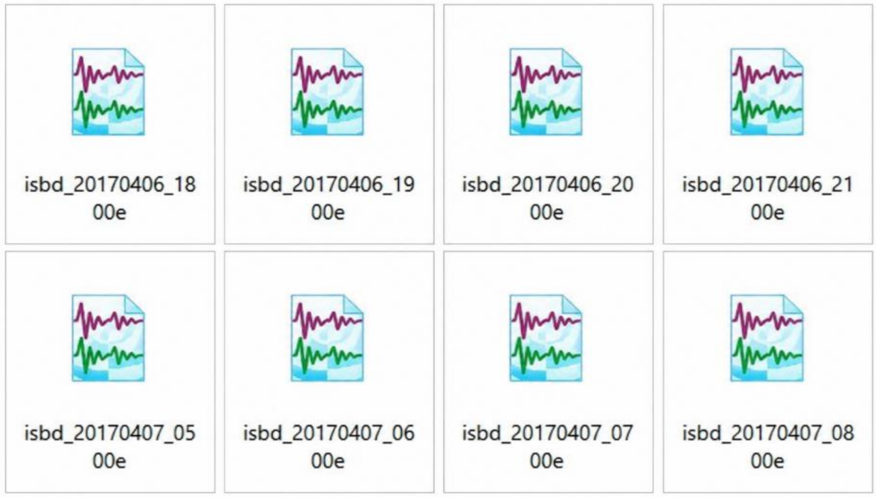

Figure 3.1. Raw Seismograms in East-West axis.

3.4 Sorting of Data

The data that is initially present in three separate folders with respect to their axes, is then sorted according to their date and time. This sorting of data provides us with a clear picture of an event and makes the earthquakes easy to identify.

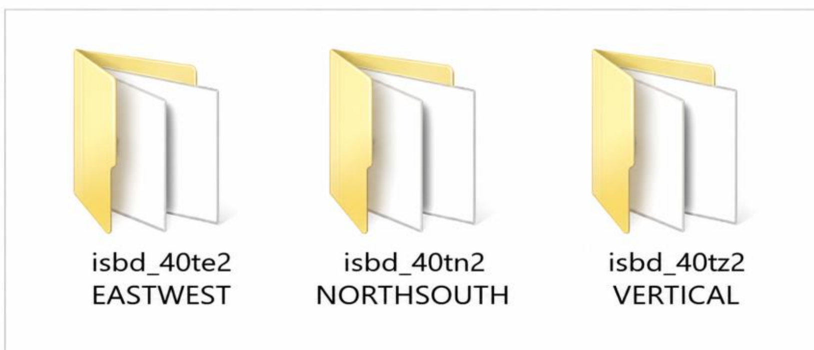

Figure 3.2. Data in three separate folders w.r.t. their axis.

The time and dates of each seismogram is plotted as it is being recorded. These seismograms have a time window of one hour. Therefore, a huge amount of data from April 2017 to July 2017 was compiled, sorted, and thoroughly checked.

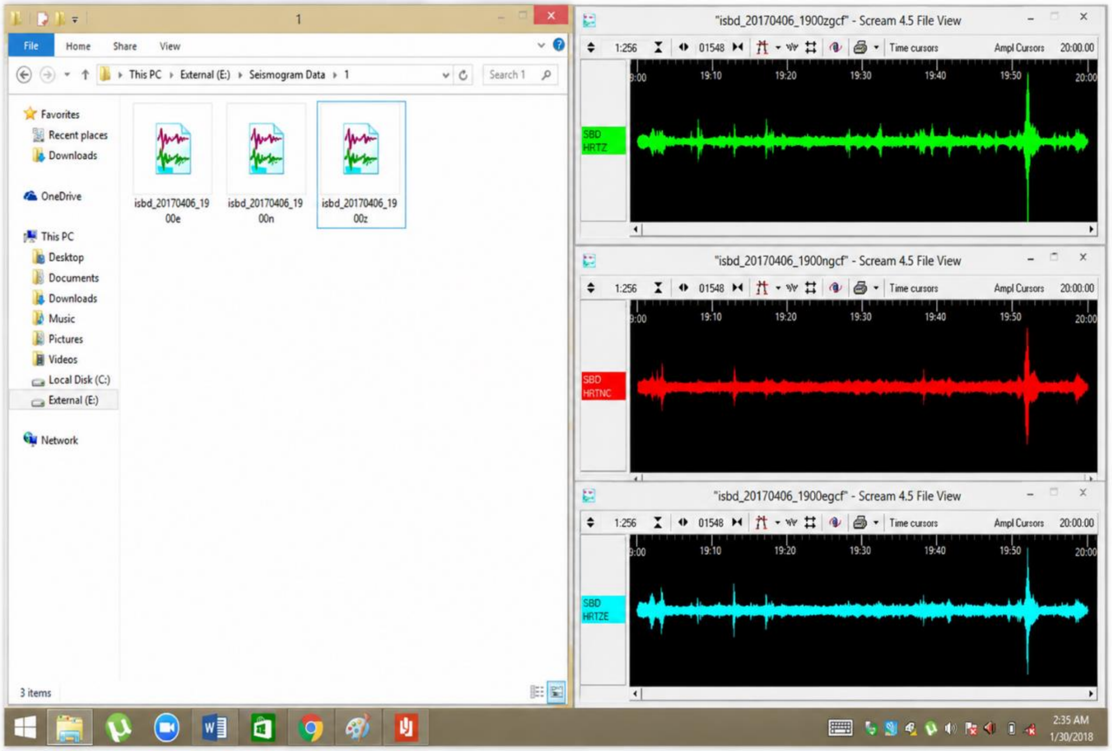

Figure 3.3. Data in separate file windows.

The seismograms were selected based on their recording date and time. The three corresponding GCF files representing the North–South, East–West, and Vertical components were then combined by selecting them simultaneously and opening them in Scream 4.5 using the "View with Scream" option.

This process displayed all three components in a single window instead of separate windows, making it easier to examine and compare the waveform data for the same seismic event. The combined view used for interpretation is shown in Figure 3.4.

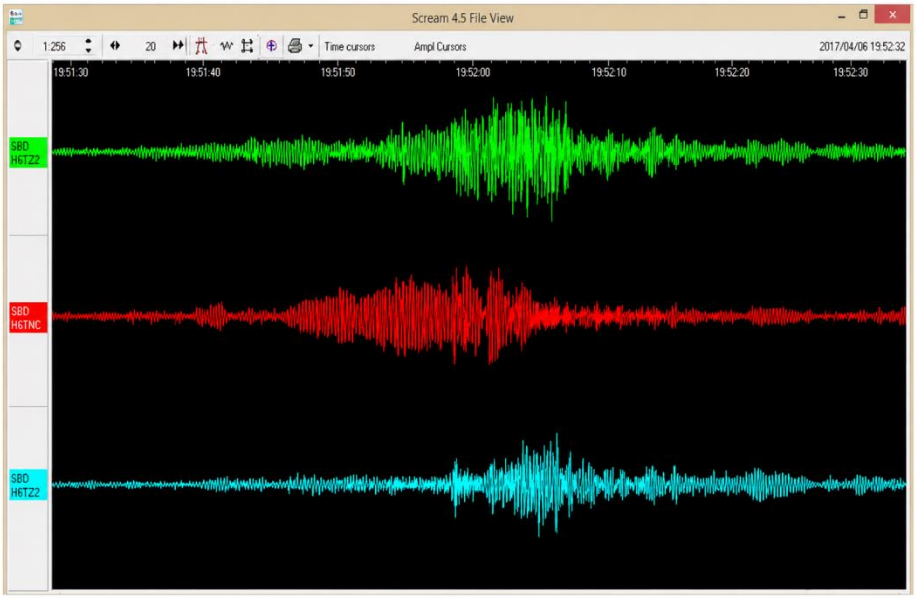

Figure 3.4. Three axes files viewed in the same window.

Instead of selecting all three files, the three files can also be saved as a single file so that all three axes could be accessed by a single click. To do so, first the files are opened as mentioned before, and then the required part is cropped out of the seismogram by dragging the cursor while keeping the “shift” key pressed.

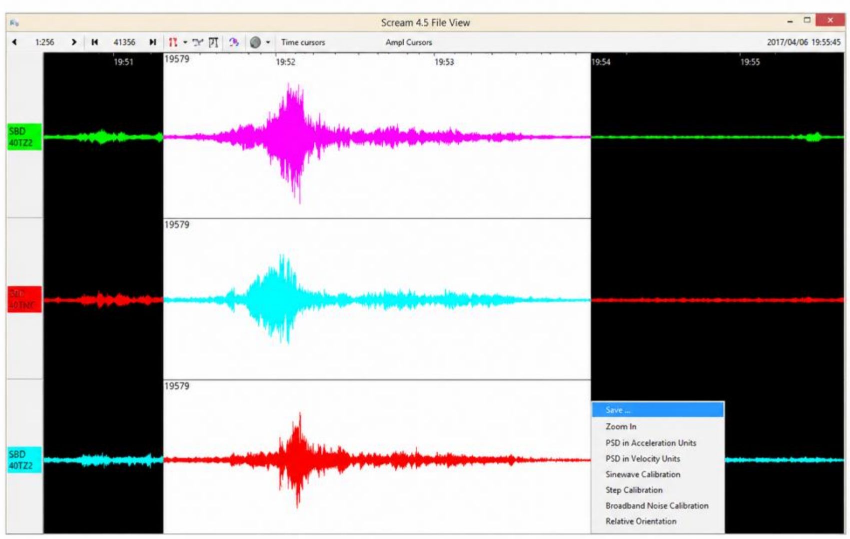

Figure 3.5. Cropping out the desired part and saving it as a single file for ease of access.

3.5 Tracing the Event

Tracing an event is tough but crucial. Seismograms, a mix of signals and background noise, help us understand what happened. In this context, the signal is an earthquake. P-waves and S-waves create a special pattern, the only way to tell them apart from noise. Noise, like wind or traffic, can make the seismograph vibrate. During an earthquake, the fastest waves, P-waves, are usually recorded first. They're the initial, bigger wiggles. S-waves come next, usually larger than P-waves. If a seismogram shows no S-waves, it means the earthquake was on the opposite side of the Earth since S-waves can't go through the liquid layer. Surface waves (Love and Rayleigh), often bigger, show up later due to their lower frequency. They reach the seismograph just after S-waves because they travel a bit slower. In shallow earthquakes, the strongest waves on the seismograph are usually surface waves.

Eight events were traced using the above-mentioned technique and these events were of and around the vicinity of Pakistan.

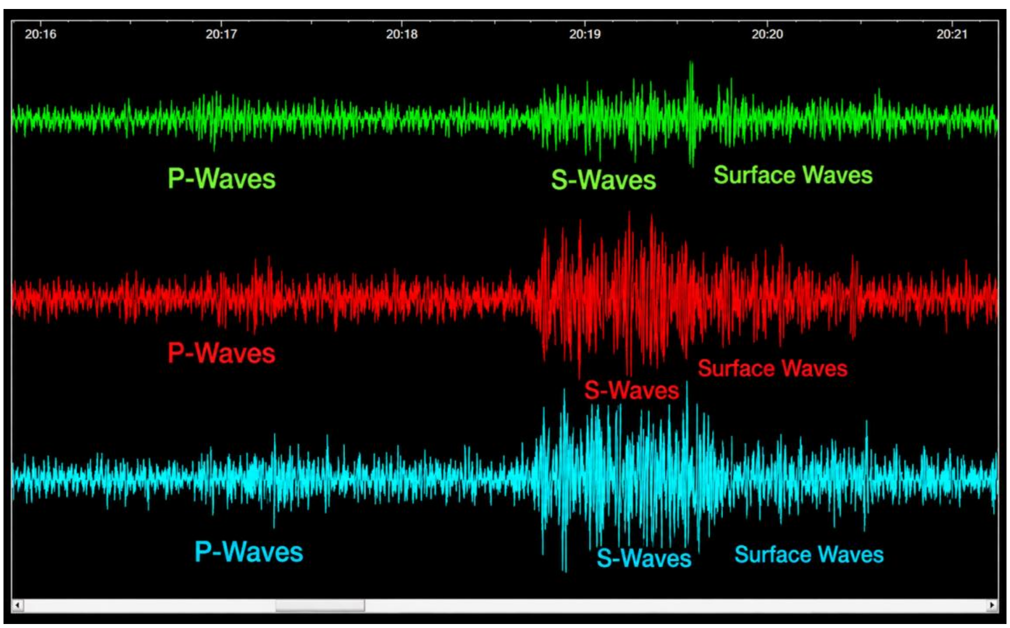

Figure 3.6. Tracing an event based on wave pattern.

3.6 Separation from Noise

The refinement of the signal is done in this step and to do so, the band pass filter is applied. Scream 4.5 offers a wide range of filters but the filter used in this research is the band-pass filter. The filter is configured with a low-pass frequency set at 1.0 hertz and a high-pass frequency set at 0.1 hertz. After the application of the filter the waveform data appears to be reduced. This reduction in the amplitude can be magnified using the arrow keys (Left for spreading the waves, right for compressing the waves, up for amplifying the amplitude and down to reduce the amplitude). It is hard to separate an event from the noise without applying the band-pass filter because the entire seismogram seems to be distorted and the event is divulged in the noise while unnecessary disfiguring of waves is present.

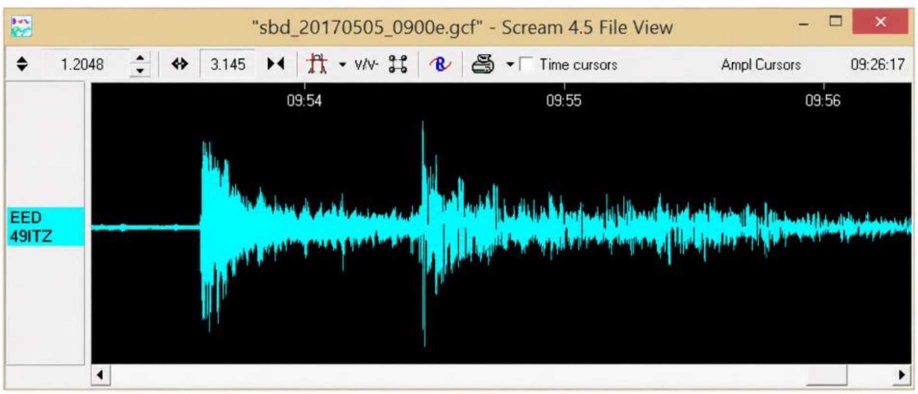

Figure 3.7.A non-filtered event.

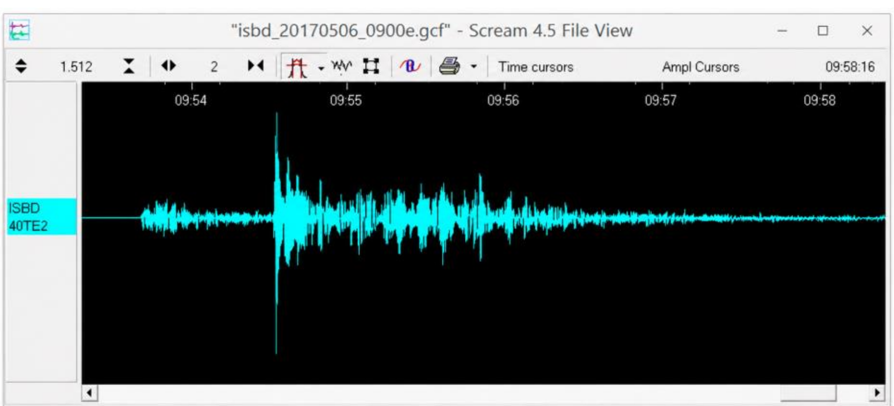

Figure 3.8.A filtered event

3.7 Calculating P and S Arrivals

The determination of P-wave and S-wave arrival times is one of the most important steps in seismogram interpretation. Accurate identification of these arrivals forms the basis for calculating several key earthquake parameters, including epicentral distance, travel time, focal depth, slowness, and residual time. Since these parameters are essential for locating and characterizing an earthquake, careful picking of the arrival times is required to minimize errors in the subsequent analysis.

The seismic waveform data were analyzed using Scream 4.5 software. Each seismic event was displayed simultaneously on the North–South, East–West, and Vertical components to ensure accurate identification of the seismic phases. The P-wave is recognized as the first arrival on the seismogram and is generally identified by the first clear deviation from the background noise. Owing to its higher propagation velocity, the P-wave reaches the seismic station before any other seismic phase. The S-wave arrives after the P-wave and is usually characterized by a larger amplitude and more pronounced ground motion.

To determine the arrival times, the cursor was placed at the first noticeable break corresponding to the onset of the P-wave and then dragged to the first significant change representing the arrival of the S-wave. The software automatically displays the time difference between these two arrivals, known as the S–P time. In the example shown in Figure 20, the measured S–P time is 18.839 seconds.

The S–P time is a critical parameter in earthquake location because it provides an estimate of the distance between the seismic station and the earthquake epicenter. As the distance from the source increases, the difference between the arrival times of the P- and S-waves also increases due to their different propagation velocities. Consequently, larger S–P times indicate that the earthquake occurred farther from the recording station. This information is subsequently used to estimate the epicentral distance and contributes to the accurate determination of earthquake location.

The S–P time is one of the most important parameters used in earthquake location. Because P-waves travel faster than S-waves, the difference between their arrival times increases with increasing distance from the earthquake source. Therefore, a larger S–P time indicates that the epicenter is located farther from the recording station, whereas a smaller S–P time suggests that the earthquake occurred relatively close to the station. Using the measured S–P times from multiple seismic stations, the epicentral location of an earthquake can be determined with greater accuracy.

In addition to estimating epicentral distance, accurately identified P- and S-wave arrivals serve as the foundation for all subsequent waveform analyses performed in this study. These arrival times are required for calculating travel-time residuals, determining wave velocities, and performing advanced analyses such as Horizontal to vertical (H/V) spectral ratio analysis and Frequency–Wavenumber (F-K) analysis. Consequently, precise phase picking is essential for obtaining reliable and meaningful results throughout the seismic waveform interpretation process.

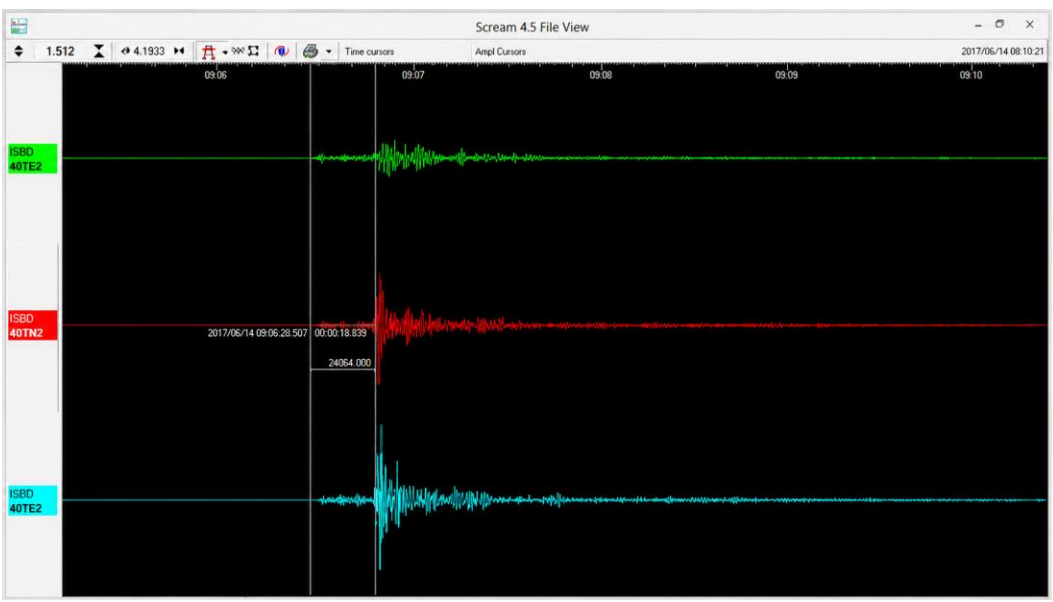

Figure 3.9 P and S arrivals and S-P window.

3.8 Calculating the Duration and Distance of the Event

The second step in the seismogram interpretation is calculating the duration of the event and the distance between the source and station. Scream 4.5 is used again for the calculation of the duration of an event. Similar methodology is applied in this step as well, the time window is generated but instead of isolating the P-waves, the entire event is marked. This entire plotting of the time window on the event will give the duration of the earthquake (4 minutes 21.250 seconds in this example) (Figure. 3.10)

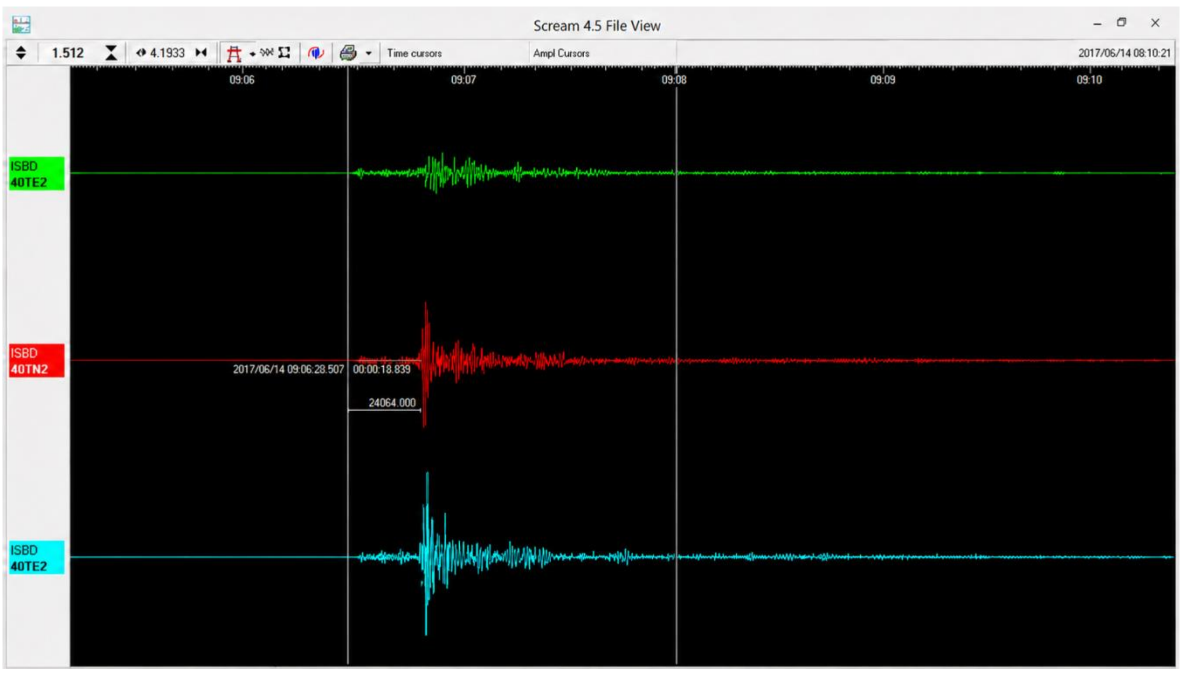

Figure 3.10. Duration of the event plotted by the time window.

For the distance calculation, the coordinates of the station and the coordinates of the source of the event are subtracted. This subtraction will give us the path of displacement from source point to the seismic station.

3.9 Calculating observed and theoretical P-Wave travel time

P-waves are the first to reach the seismograph and they carry the most useful information. These waves can pass through solids as well as liquids but apart from that, They are also quite important in seismological studies. P-waves travel time is dependent upon the depth of the source of generation. For a specific depth, The P-waves' observed travel time is recorded.

For the P-waves' hypothetical travel time, a standard iasp91 velocity model is given where velocities of P-waves are plotted against a specific depth of source. From there, the velocity of P-waves is noted and as the source-station distance is known, the travel time of P-waves can be calculated. Note that this travel time is different from the observed travel-time.

3.10 Calculating Residual (R.M.S.) and Ray Parameter

The primary goal of this study is to evaluate each seismic station's data quality. The residual values that are left behind after deducting the P-waves' theoretical and observed travel periods are used to assess the quality of the data. The recorded data is of low quality if there is a larger discrepancy between the observed and theoretical journey times. On the other hand, the data quality will improve with a lower residual.

Ray Parameter or the “Slowness” of the wave is the reciprocal of its apparent velocity. The geometric characteristic of a seismic ray that doesn't change along its course is called the ray parameter. All that is needed to determine the ray parameter is to add the residual root mean square (R.M.S) to the measured P-wave travel time.

3.11 H/V horizontal to vertical Analysis to Generate Noise Spectrum.

The horizontal to vertical spectral ratio, or H/V (Horizontal to Vertical), is a quick and easy method for obtaining site parameters of technical importance. It measures the ambient noise wave field on the surface of the ground using a single, three-component sensor. (Hirono, Mayuko, & Kohji, 2004), (Donat, Fortunat, and Domenico (2004). Several modeling techniques are used to simulate the H/V curve, and these techniques may have an impact on the retrieved soil profile. A three-component sensor that is positioned on the ground's surface and records the seismic noise wave field is used to collect the data. Geopsy is used to calculate the Fourier spectra of the recorded seismic noise for each of the three components.

Geopsy is a graphical user interface for organizing, viewing, and processing geophysical signals. Geopsy is a database used to gather all information about recorded signals. GCF files are not supported by Geopsy; therefore, they should be converted in SAC format. For that, gcf2sac converter is used. There are two ways in which the files can be converted, either select the desired events (in GCF) and drag and drop them on the gcf2sac conversion file (figure 23) or convert the entire GCF data in SAC by a single command. To do so:

a) DOS is opened.
b) GCF data folder is accessed by the command, “cd <folder name>”
c) To check for the entire GCF file in the folder, “DIR” command is used.
d) To select the .GCF files, “dirf *.gcf” command is used.
e) For the conversion of GCF data into SAC, “gursei” command is used.

The signals are then converted into SAC format that is easily supported by Geopsy.

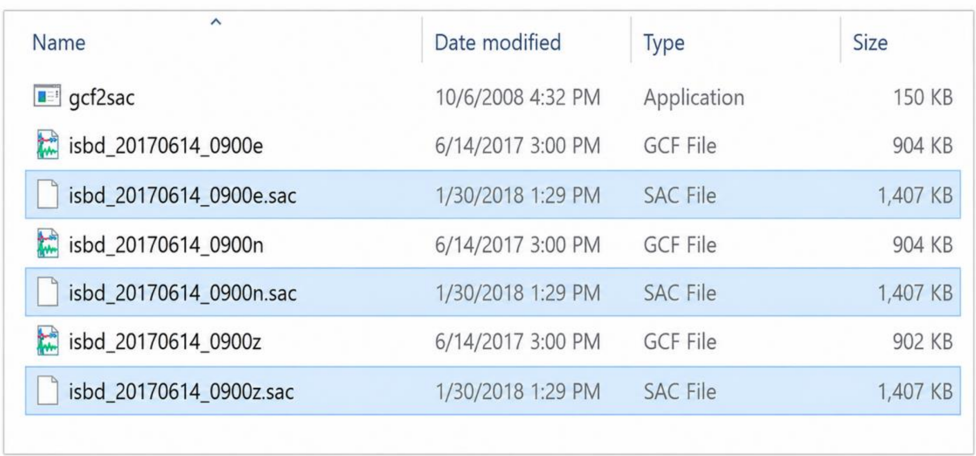

Name	Date modified	Type	Size
gcf2sac	10/6/2008 4:32 PM	Application	150 KB
isbd_20170614_0900e	6/14/2017 3:00 PM	GCF File	904 KB
isbd_20170614_0900e.sac	1/30/2018 1:29 PM	SAC File	1,407 KB
isbd_20170614_0900n	6/14/2017 3:00 PM	GCF File	904 KB
isbd_20170614_0900n.sac	1/30/2018 1:29 PM	SAC File	1,407 KB
isbd_20170614_0900z	6/14/2017 3:00 PM	GCF File	902 KB
isbd_20170614_0900z.sac	1/30/2018 1:29 PM	SAC File	1,407 KB

Figure 3.11.GCF files converted in SAC using gcf2sac convertor.

These SAC files are then accessed by using Geopsy database. These files are then loaded in the processing window.

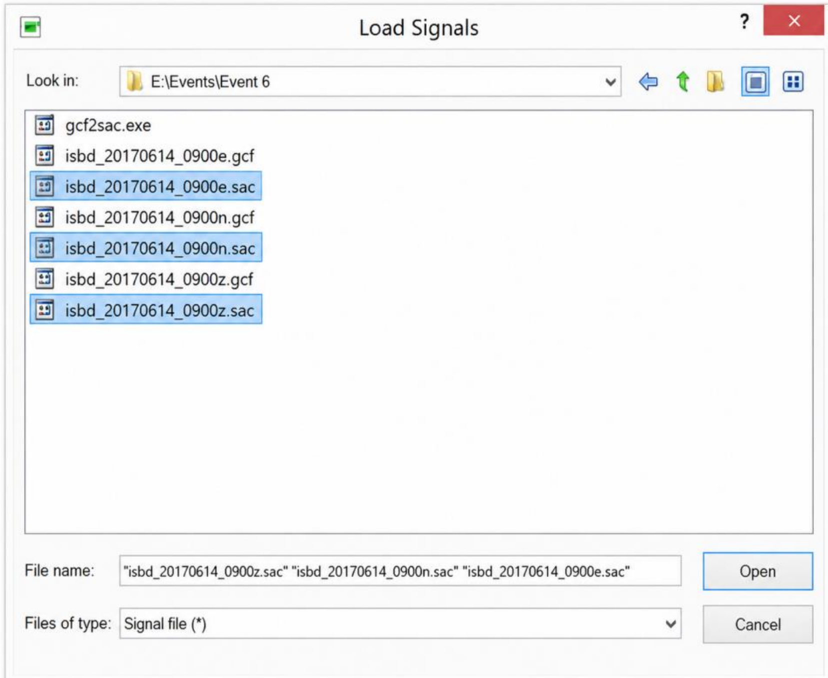

Figure 3.12. Loading of signals in Geopsy.

After the signals are loaded in Geopsy, the SAC files are selected and with the right click of the mouse the H/V (Horizontal to vertical) analysis is selected.

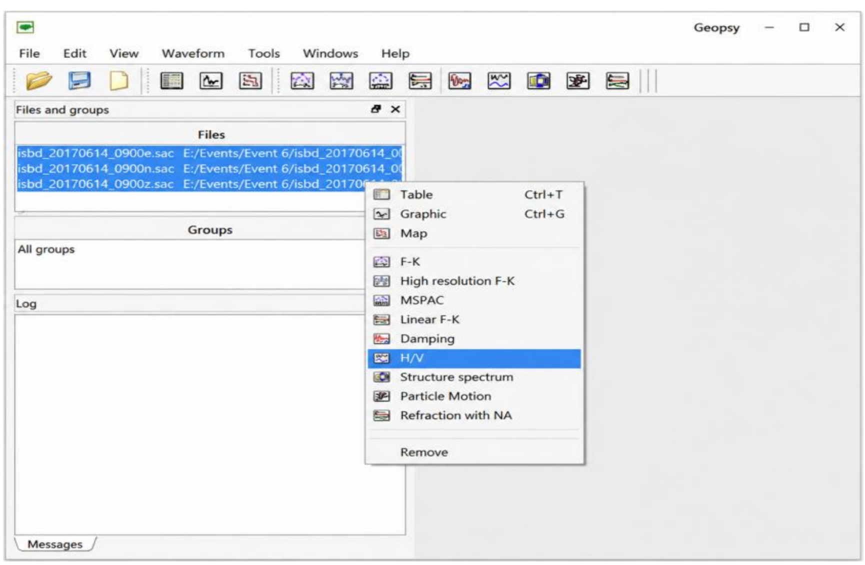

Figure 3.13. Selection of H/V (Horizontal to Vertical) .

First, the signals are shown in the form of waves and a parameter-processing window is opened. Filters can be added or removed as per requirement.

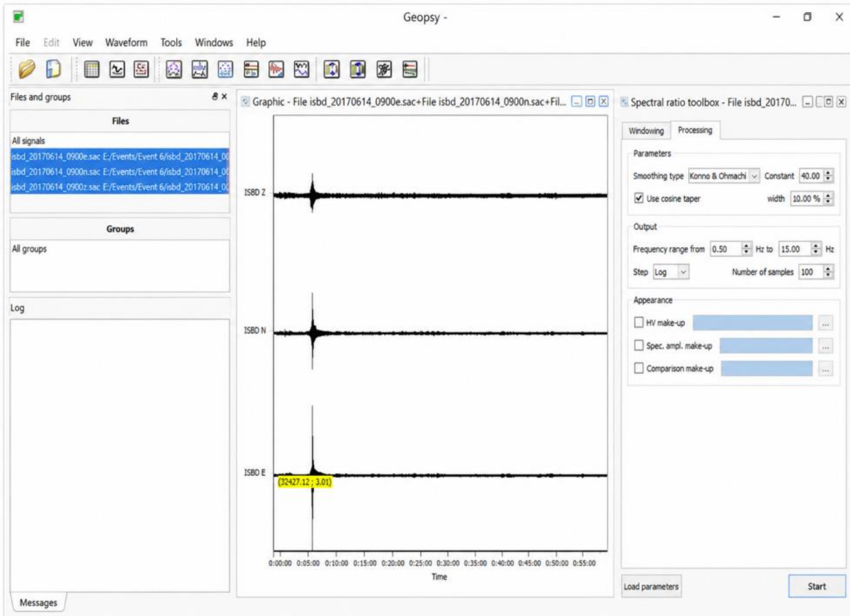

Figure 3.14. Waveform view in Geopsy.

After clicking the “Start” button located at the bottom-right corner of the software interface, the spectrum is generated. The resulting spectrum provides a graphical representation of the frequency content of the selected seismic signal, allowing detailed examination of its spectral characteristics. The generated spectrum consists of a solid black line representing the main spectral signal, dotted lines indicating the possible standard deviation or confidence limits, and several colored lines corresponding to different spectral components or processing results. These graphical elements help assess the quality of the seismic data and identify the dominant frequency ranges present in the recorded waveform.

CHAPTER 4
EVENTS INTERPRETATION

4.1 Interpreted Events

The same events that were recorded in Islamabad, Lahore and Peshawar seismic stations had to be chosen and they depicted some residual root mean square (R.M.S). These events were then sorted according to their respective seismic stations and the data that was calculated in interpretation was then complied. These events are displayed individually with respect to their respective seismic recording stations.

Sr. No.	Date	Time (UTC)	Lat. (N)	Long. (E)	Depth (Km)	Magnitude	Region
1	2017-07-08	10:12:33	34.680	73.380	40	4.8	Pakistan
2	2017-05-06	09:52:29	36.670	71.550	198	5.2	Hindukush, Afghanistan
3	2017-04-22	19:37:36	29.700	67.480	15	4.4	Pakistan
4	2017-07-20	14:04:43	36.460	71.150	187	4.0	Hindukush, Afghanistan
5	2017-06-14	09:06:09	34.900	72.870	54	4.6	Pakistan
6	2017-05-16	18:13:32	36.720	71.500	175	4.2	Hindukush, Afghanistan

Sr.no.	Date	Time UTC	Lat. (N)	Long. (E)	Depth (Km)	Magnitude	Region
7	2017-07-09	11:35:28	27.500	64.830	49	4.7	Southwest Pakistan
8	2017-07-08	22:13:53	24.080	65.170	10	4.1	Off-coast Pakistan

4.2 Calculated Parameters for Islamabad Station

These same events were recorded at the Lahore seismic station and the parameters were calculated using the same methodology. Below is the list of all events in a single table.

Sr. No.	P-Arrival	S-Arrival	S – P	P-wave travel time(obs.)	P-wave travel time(th.)	Ray Parameter	(R.M.S)
1	10:12:51	10:13:07	16 s	18 s	13.53 s	22.47 s	4.47 s
2	09:53:35	09:54:27	52 s	66 s	42.87 s	89.13 s	23.13 s
3	19:39:17	19:40:32	75 s	101 s	84.49 s	115.51 s	14.51 s
4	14:05:57	14:06:16	19 s	74 s	43.09 s	106.99	31.99 s
5	09:06:28	09:06:45	17 s	19 s	16.39 s	21.60 s	2.60 s

Sr. No.	P-Arrival	S-Arrival	S – P	P-wave travel time(obs.)	P-wave travel time(th.)	Ray Parameter	(R.M.S)
6	18:14:26	18:14:56	30 s	54 s	44.38 s	63.62 s	9.62 s
7	11:37:45	11:39:17	92 s	137 s	134.86 s	139.14 s	2.14 s
8	22:17:19	22:18:44	86 s	216 s	194.25	237.75	21.75

4.3 Calculated Parameters for Lahore Station

These same events were recorded at the Lahore seismic station and the parameters were calculated using the same methodology. Below is the list of all events in a single table.

Sr. No.	P-Arrival	S-Arrival	S – P	P-wave travel time(obs.)	P-wave travel time(th.)	Ray Parameter	(R.M.S)
1	10:13:01	10:13:23	22 s	28 s	43.84	43	15
2	09:53:48	09:54:59	71 s	79 s	74.258	83.742	4.742
3	19:39:31	19:40:51	80 s	155 s	84.873	145.127	30.127
4	14:06:09	14:06:47	38 s	86 s	74.81	101.19	15.19
5	09:06:58	09:07:19	21 s	49s	48.395	59.605	10.605
6	18:14:41	18:15:20	39 s	69s	76.244	76.244	7.244
7	11:38:02	11:39:54	112 s	154 s	126.77	181.23	27.239
8	22:17:51	22:19:24	93 s	238s	179.85	296.15	58.151

4.4 Calculated Parameters for Peshawar Station

Sr. No.	P-Arrival	S-Arrival	S - P	P-wave travel time(obs.)	Ray Parameter	(R.M.S)	P-wave travel time(th.)
1	10:13:07	10:13:27	20 s	34 s	45.49 s	11.49	22.51 s
2	09:53:38	09:54:35	57 s	69 s	102.497 s	27.50	35.503 s
3	19:39:49	19:40:57	76 s	133 s	191.68 s	38.68	74.32 s
4	14:06:55	14:07:16	21 s	132 s	130.471 s	36.47	33.529 s
5	09:07:00	09:07:23	23 s	51 s	82.903 s	19.93	19.097 s
6	18:14:51	18:15:23	32 s	80 s	123.267 s	13.27	36.733 s
7	11:38:46	11:40:30	104 s	217 s	289.347 s	29.35	120.653 s
8	22:18:03	22:19:24	86 s	250 s	313.524 s	43.53	186.47 s

4.5 Generation of H/V horizontal to vertical Spectrum of the Events Recorded at Islamabad Seismic Station

This instrument measures the spectral ratios of horizontal to vertical (H/V) vibrations from any kind of vibration signal, including earthquake and ambient vibrations. H/V horizontal to vertical analysis is performed on the events that were traced from the available data of Islamabad station. These events contained noise as well as the traces of the event. To distinguish noise from signal.

4.6 Event 1 H/V (Horizontal to Vertical) Spectrum

H/V (Horizontal to Vertical) analysis of the first event was performed. Figure (4.1) displays each elements' H/V (Horizontal to Vertical) spectrum.

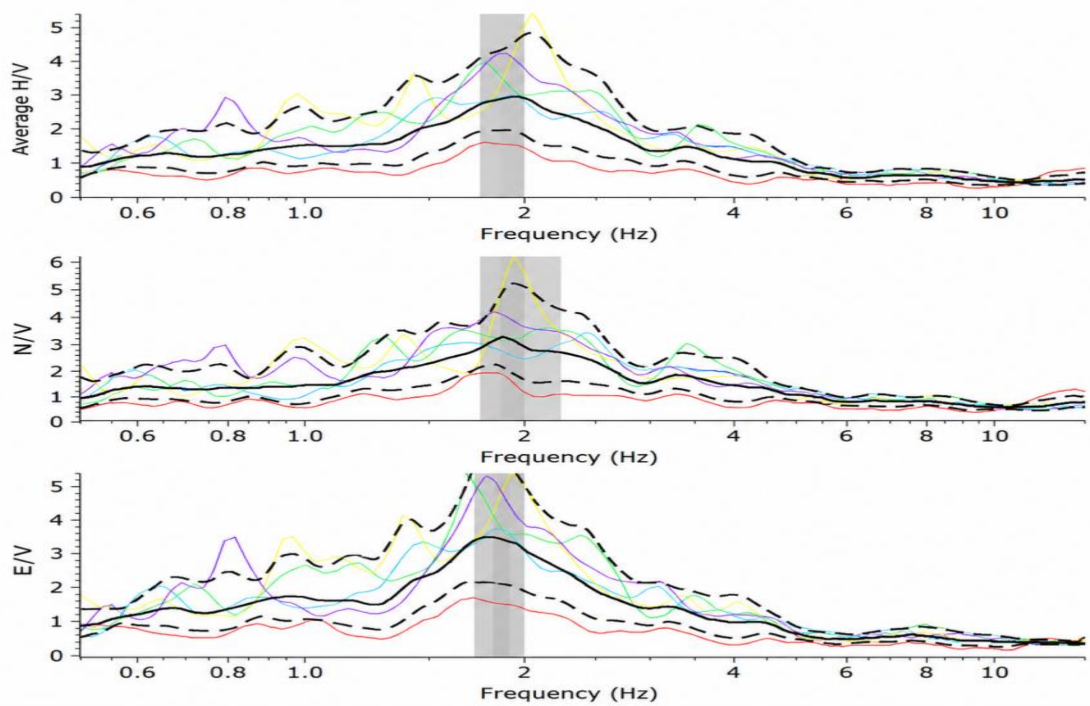

Figure 4.1. Event 1 H/V horizontal to vertical spectrum for seismic station.

The H/V horizontal to vertical mathematically averaged overall colored individual H/V horizontal to vertical curves are shown by the black bar. The two lines with dashes on this graph represent the peak frequency and average deviation. The frequency value is on the edge of the vibrant and dark greys. The surrounding noise is depicted by the colored lines. In this case, the H/V horizontal to vertical maximum frequency's minimum average Deviation is fo = 1.855, while its highest average deviation is fo = 1.947. Ao=3.55 is the value of the H/V horizontal to vertical Max. average amplitude

4.7 Event 2 (H/V horizontal to vertical Spectrum)

H/V horizontal to vertical analysis of the second event was performed. Figure (4.2) Displays the H/V horizontal to vertical Spectrum of all the elements.

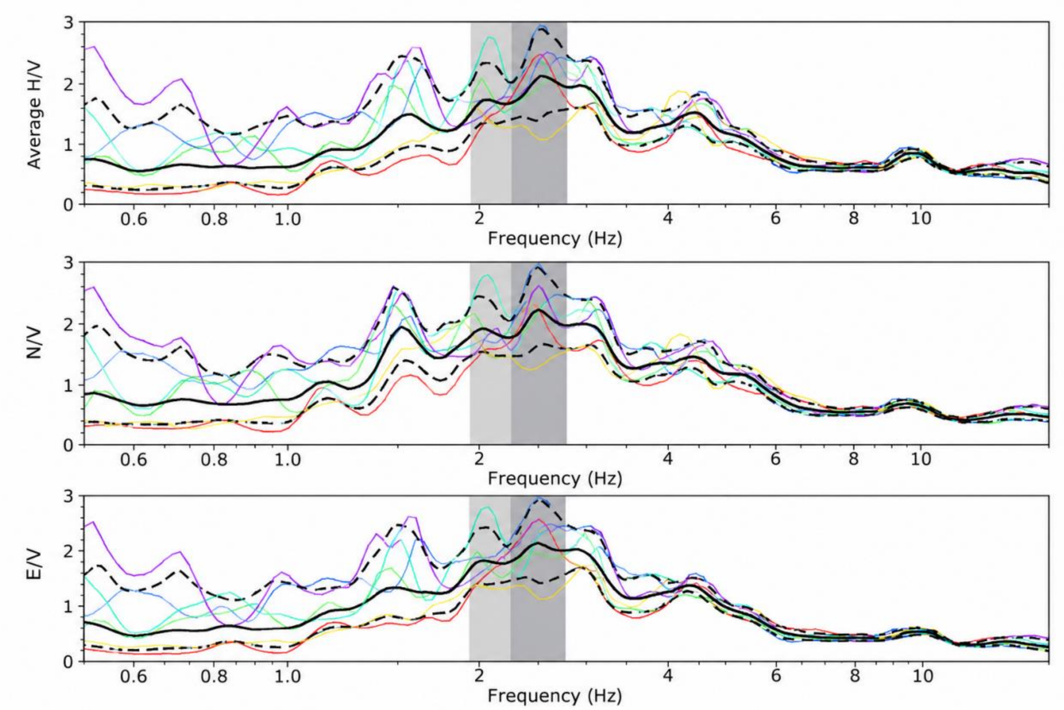

Figure 4.2. Event 2 H/V horizontal to vertical spectrum for seismic station.

H/V horizontal to vertical mathematically averaged overall colored individual H/V horizontal to vertical curves are shown by the black bar. The two lines with dashes on this graph represent the peak frequency and average deviation. The frequency value is on the edge of the vibrant and dark greys. The surrounding noise is depicted by the colored lines. In this case, the H/V horizontal to vertical maximum frequency's minimum average Deviation is fo = 1.610, while its highest average deviation is fo = 1.613, Ao=3.11 is the value of the H/V horizontal to vertical average peaked amplitude.

4.8 Event 3 H/V (HORIZONTAL TO VERTICAL) spectrum

H/V horizontal to vertical analysis of the third event was performed. Figure (4.3) shows the H/V horizontal to vertical spectrum of all the components.

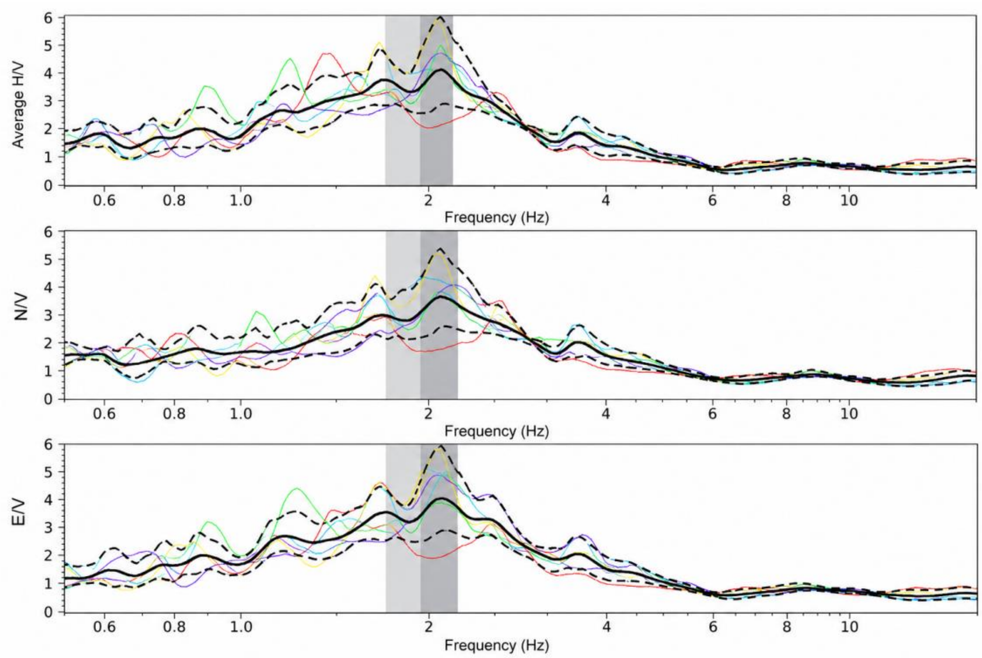

Figure 4.3. Event 3 H/V (HORIZONTAL TO VERTICAL) spectrum for seismic station.

H/V horizontal to vertical mathematically averaged overall colored individual H/V horizontal to vertical curves are shown by the black bar. The two lines with dashes on this graph represent the peak frequency and average deviation. The frequency value is on the edge of the vibrant and dark greys. The surrounding noise is depicted by the colored lines. In this case, the H/V horizontal to vertical maximum frequency's minimum average Deviation is fo = 2.473, while its highest average deviation is fo = 2.274, Ao=2.77 is the value of the H/V horizontal to vertical average peaked amplitude.

4.9 Event 4 H/V horizontal to vertical spectrum

H/V horizontal to vertical analysis of the fourth event was performed. Figure (4.4) shows the H/V horizontal to vertical spectrum of all the components.

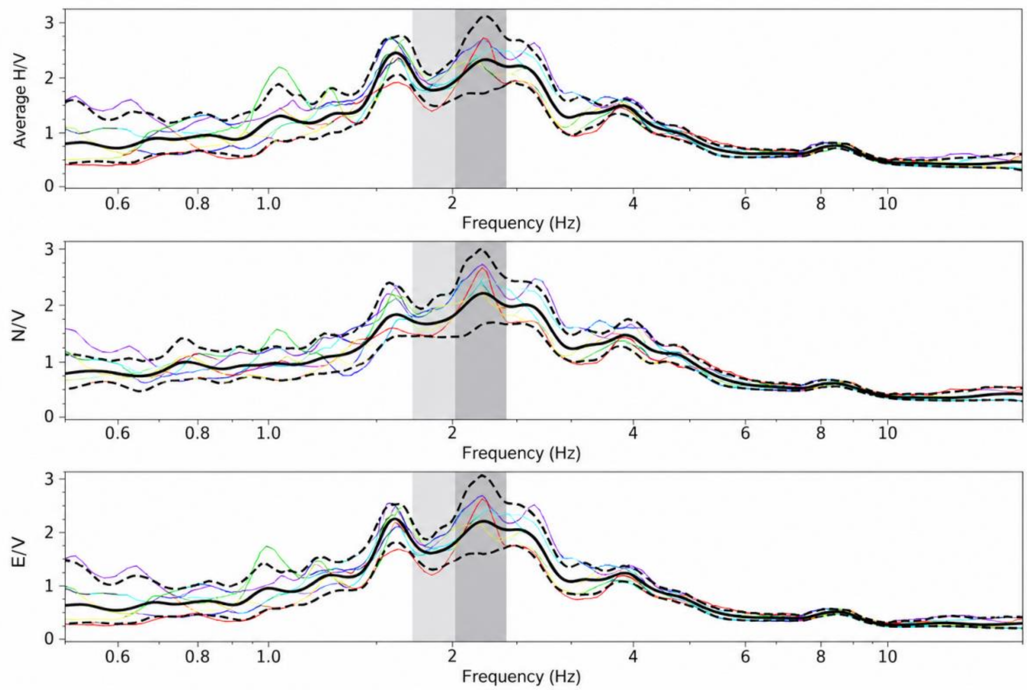

Figure 4.4. Event 4 H/V horizontal to vertical spectrum for seismic station.

H/V horizontal to vertical mathematically averaged overall colored individual H/V horizontal to vertical curves are shown by the black bar. The two lines with dashes on this graph represent the peak frequency and average deviation. The frequency value is on the edge of the vibrant and dark greys. The surrounding noise is depicted by the colored lines. In this case, the H/V horizontal to vertical maximum frequency's minimum average Deviation is fo = 2.398, while its highest average deviation is fo = 2.404, Ao=2.92 is the value of the H/V horizontal to vertical average peaked amplitude.

4.10 Event 5 H/V horizontal to vertical spectrum

H/V horizontal to vertical analysis of the fifth event was performed. Figure (4.5) shows the H/V horizontal to vertical spectrum of all the components.

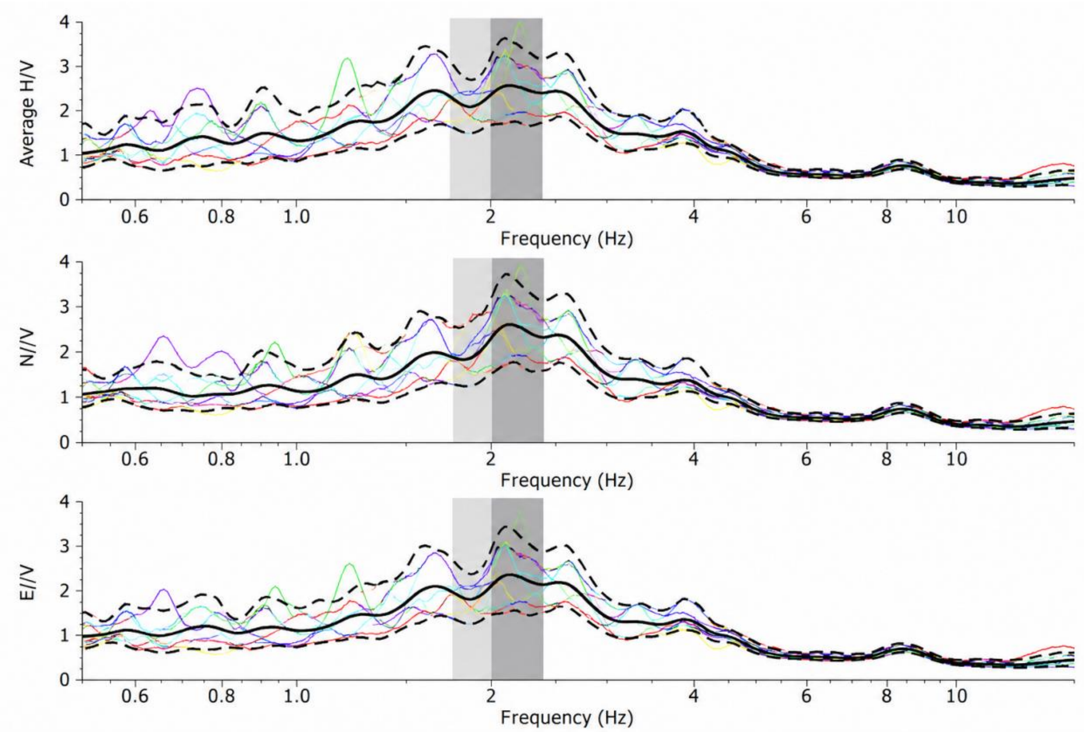

Figure 4.5. Event 5 H/V horizontal to vertical spectrum for seismic station.

H/V horizontal to vertical mathematically averaged overall colored individual H/V horizontal to vertical curves are shown by the black bar. The two lines with dashes on this graph represent the peak frequency and average deviation. The frequency value is on the edge of the vibrant and dark greys. The surrounding noise is depicted by the colored lines. In this case, the H/V horizontal to vertical maximum frequency's minimum average Deviation is fo = 1.905, while its highest average deviation is fo = 1728, Ao=3.47 is the value of the H/V horizontal to vertical average peaked amplitude.

4.11 Event 6 H/V horizontal to vertical spectrum

H/V horizontal to vertical analysis of the sixth event was performed. Figure (4.6) shows the H/V horizontal to vertical spectrum of all the components.

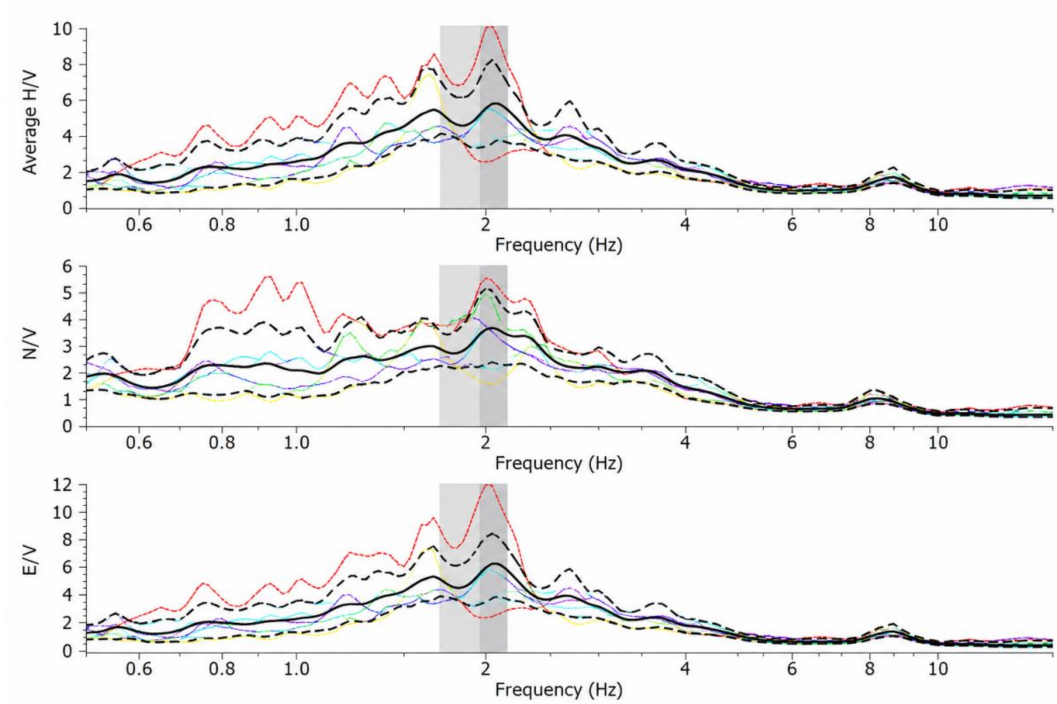

Figure 4.6. Event 6 H/V horizontal to vertical spectrum for seismic station.

H/V horizontal to vertical mathematically averaged overall colored individual H/V horizontal to vertical curves are shown by the black bar. The two lines with dashes on this graph represent the peak frequency and average deviation. The frequency value is on the edge of the vibrant and dark greys. The surrounding noise is depicted by the colored lines. In this case, the H/V horizontal to vertical maximum frequency's minimum average Deviation is fo = 2.284, while its highest average deviation is fo = 2.387, Ao=2.287 is the value of the H/V horizontal to vertical average peaked amplitude.

4.12 Event 7 H/V horizontal to vertical spectrum

H/V horizontal to vertical analysis of the seventh event was performed. Figure (4.7) shows the H/V horizontal to vertical spectrum of all the components.

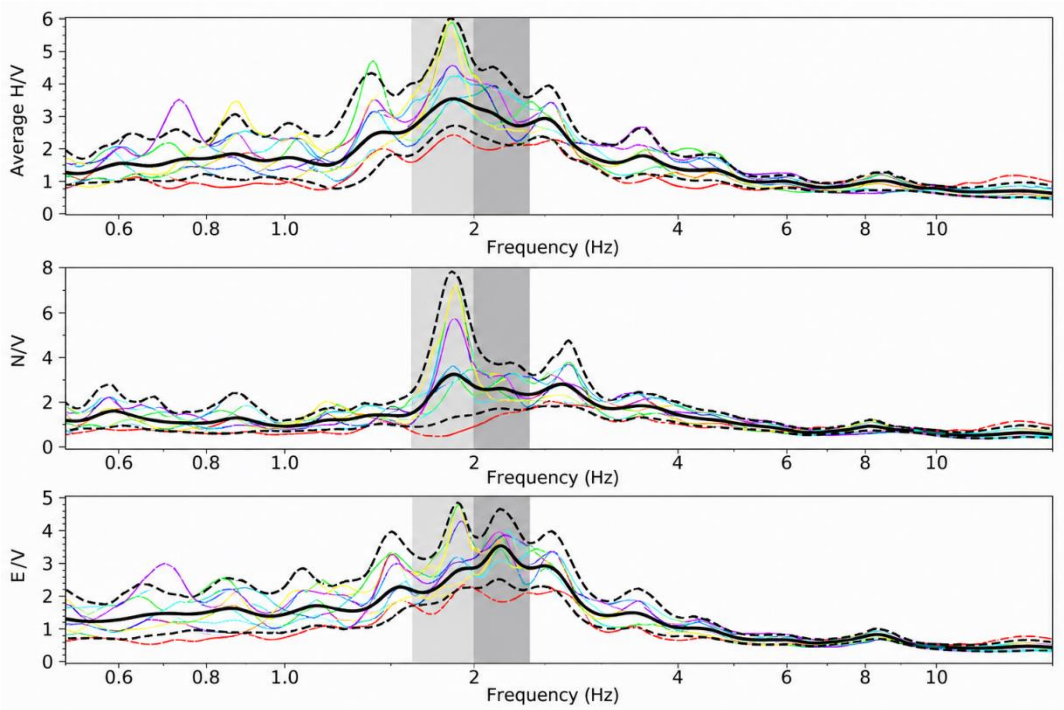

Figure 4.7. Event 7 H/V horizontal to vertical spectrum for seismic station.

H/V horizontal to vertical mathematically averaged overall colored individual H/V horizontal to vertical curves are shown by the black bar. The two lines with dashes on this graph represent the peak frequency and average deviation. The frequency value is on the edge of the vibrant and dark greys. The surrounding noise is depicted by the colored lines. In this case, the H/V horizontal to vertical maximum frequency's minimum average Deviation is fo = 2.632, while its highest average deviation is fo = 2.147, Ao=2.59 is the value of the H/V horizontal to vertical average peaked amplitude.

4.13 Event 8 H/V horizontal to vertical spectrum

H/V horizontal to vertical analysis of the seventh event was performed. Figure (4.8) shows the H/V horizontal to vertical spectrum of all the components.

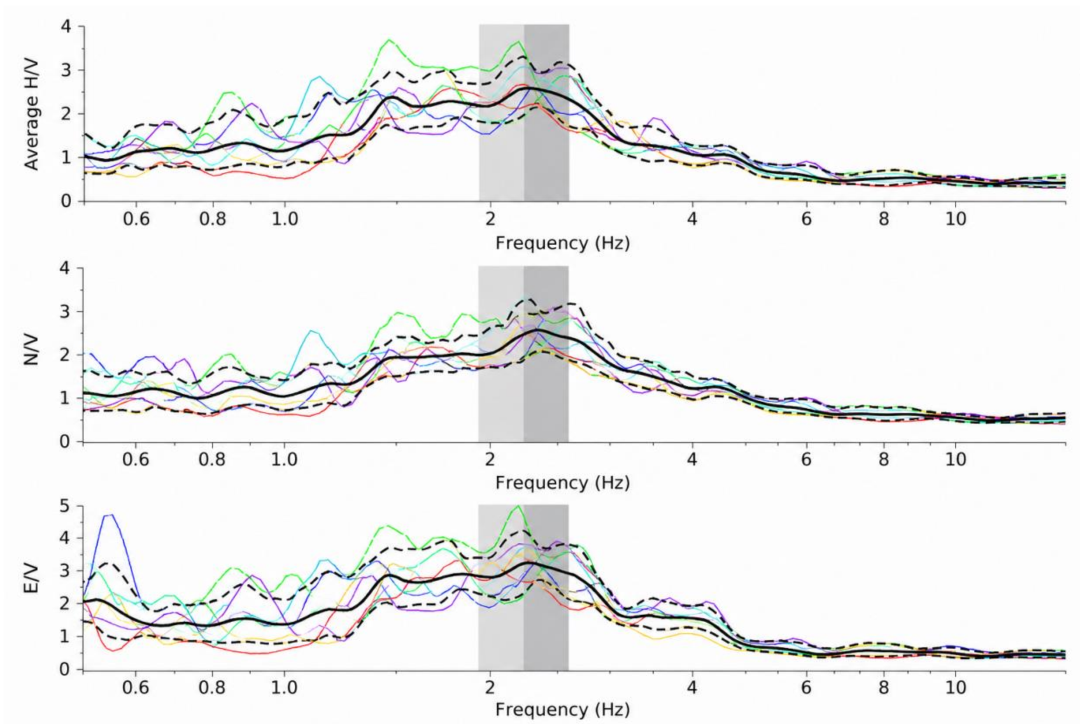

Figure 4.8. Event 8 H/V horizontal to vertical spectrum for seismic station.

H/V horizontal to vertical mathematically averaged overall colored individual H/V horizontal to vertical curves are shown by the black bar. The two lines with dashes on this graph represent the peak frequency and average deviation. The frequency value is on the edge of the vibrant and dark greys. The surrounding noise is depicted by the colored lines. In this case, the H/V horizontal to vertical maximum frequency's minimum average Deviation is fo = 2.441, while its highest average deviation is fo = 2.473, Ao=2.86 is the value of the H/V horizontal to vertical average peaked amplitude.

4.14 Results

The residual error is computed by contrasting the actual travel time of P-waves with their expected theoretical travel time. This error basically shows the time delay and slowness in the P-wave arrival. This time delay indicates the hindrance that comes across the path of P-waves. Residual errors from all three stations were calculated and sorted out. These residuals were calculated, and the total error generated from all three seismic stations of Islamabad, Lahore and Peshawar was compared.

Sr. No.	**Islamabad (R.M.S.)**	**Lahore root mean square (R.M.S)**	**Peshawar root mean square (R.M.S)**
1.	4.47	15.00	11.49
2.	23.13	4.74	27.50
3.	14.51	30.13	38.68
4.	32.10	15.19	36.47
5.	2.61	10.61	19.93
6.	9.62	7.24	13.27
7.	2.14	27.24	29.35
8.	21.75	58.15	43.53
Total	110.33	168.3	220.22

CONCLUSIONS

1. Earthquake events that were traced from the provided data were dominant in two regions, the Hindukush region of Afghanistan and the Main Boundary Thrust in Pakistan.
2. The residual error calculated for all three stations portrayed variations. The total R.M.S. from Islamabad, Lahore and Peshawar seismic stations differed from each other. This difference shows that the data quality in these stations is not same.
3. Residual is a direct function of noise. Peshawar station exhibited the greatest R.M.S. values which mean that data from Peshawar station was not dependable.
4. The comparison of waveform recordings from the three seismic stations demonstrated noticeable differences in signal quality and waveform clarity, indicating that local site conditions and ambient noise significantly influence the quality of recorded seismic data.
5. The identification of P-wave and S-wave arrivals, along with the calculation of travel time, epicentral distance, and residual values, proved effective in evaluating the performance of the Pakistan Seismic Network stations and assessing the reliability of the recorded earthquake data.
6. The application of H/V horizontal to vertical spectral ratio analysis and Frequency–Wavenumber (F-K) analysis provided valuable information regarding the frequency characteristics of the recorded seismic signals, highlighting the importance of spectral analysis techniques in seismic data interpretation and earthquake monitoring.

REFERENCES

Adhami, N., Ilyas, M., and Ahmad, M. conducted seismotectonic investigations in the Rawalpindi region for the National Engineering Service of Pakistan (NESPAK) in 1980, resulting in a comprehensive report spanning 139 pages.

Bolt, B. A. authored the fourth edition of "An Introduction to the Theory of Seismology" in 1985, published by Cambridge University Press.

Capon, J., an IEEE member, in 1969, contributed to the field with a paper titled "High-Resolution Frequency-Wavenumber Spectrum Analysis," published by IEEE.

Fortunat, K., Donat, F., and Domenico, G. presented findings on array measurements of S-wave velocities from ambient vibrations at the Swiss Seismological Service in 2004.

Hussain, A., and Yeats, R. S. explored the zone of late Quaternary deformation in the southern Peshawar Basin, Pakistan, in 1989, published by the Geological Society of America.

Kazmi, A., and Jan, M. published "Geology & Tectonics of Pakistan" in 1997 through Graphic Publication.

Kohji, T., Hiroshi, A., and Mayuko, Y. shared insights on multi-dimensional VS-Profiling with Microtremor H/V horizontal to vertical and Array Techniques at the 13th World Conference on Earthquake Engineering in 2004.

Monalisa, A., and Khawaja investigated seismic zonation based on Peak Ground Acceleration (PGA) values in a part of Northern Pakistan in 2002, presented at the "ILP-Progress and Prospects" conference in Kaikoura, New Zealand.

Naseem, A., and Ghulam, M. S. conducted stratigraphic correlation and created isopach maps of the Punjab Platform in the Middle Indus Basin, Pakistan, as documented in "Search and Discovery" in 2011.

The Survey of Pakistan published the topographic map of Islamabad in 1982 with a scale of 1:50, 000.

Shah, M. A., J., I., M., Q., and Tufail, A. M. updated the design ground motion prediction for Lahore and the surrounding region of Pakistan in 2008, presented at the World Conference of Earthquake Engineering in Beijing, China, under the Micro Seismic Studies Program (MSSP).